

Application of the Piloting Law Based on Adaptive Differentiators via Second Order Sliding Mode for a Fixed Wing Aircraft

Zaouche Mohammed, Amini Mohammed, Foughali Khaled, Hamissi Aicha, Aktouf Mohand Arezki, Bouregghda Ilyes

Abstract—In this paper, we present a piloting law based on the adaptive differentiators via high order sliding mode controller, by using an aircraft in virtual simulated environment. To deal with the design of an autopilot controller, we propose a framework based on Software in the Loop (SIL) methodology and we use Microsoft™ Flight Simulator (FS-2004) as the environment for plane simulation. The aircraft dynamic model is nonlinear, Multi-Input Multi-Output (MIMO) and tightly coupled. The nonlinearity resides in the dynamic equations and also in the aerodynamic coefficients' variability. In our case, two (02) aircrafts are used in the flight tests, the Zlin-142 and MQ-1 Predator. For both aircrafts and in a very low altitude flight, we send the piloting control inputs to the aircraft which has stalled due to a command disconnection. Then, we present the aircraft's dynamic behavior analysis while reestablishing the command transmission. Finally, a comparative study between the two aircraft's dynamic behaviors is presented.

Keywords—Adaptive differentiators, Microsoft Flight Simulator, MQ-1 predator, second order sliding modes, Zlin-142.

I. INTRODUCTION

THE control of dynamical systems in presence of uncertainties and disturbances is a common problem to deal with when considering real process. The effect of these uncertainties on the dynamical systems should be carefully taken into account in the controller design phase since they can degrade the performance or even lead to a system instability. For this reason, during the recent years, the problem of controlling dynamical systems in presence of heavy uncertainty conditions has become an important research subject. As a result, considerable progress has been attained in the robust control techniques such as nonlinear adaptive control, model predictive control, backstepping, sliding mode control and others [1]-[5], [11], [19]. These techniques are able to guarantee the attainment of the control objectives in spite of modeling errors and/or uncertainties on parameters that can affect the controlled plant.

Sliding mode control is generally considered to be very robust and simple to implement, however, some reservations are expressed on such approach due to the so-called chattering phenomenon (effects of the discontinuous nature of the control), and the high control activity.

M. Zaouche is with the Technology Department, Centre de Recherche et Développement Réghaia, Algeria (phone: 00213 551391389; e-mail: zaouchemohamed@yahoo.fr).

M. Amini, K. Foughali, A. Hamissi, M. A. Aktouf and I. Bouregghda are researchers at Centre de Recherche et Développement Réghaia.

The first order sliding mode control can be a solution for this piloting problem; however, its implementation generates the chattering phenomenon [9], [10], [14] and the singularity problem. In order to avoid them, a new version of the differentiators with a dynamic adaptation of the gains via second order sliding modes approach, is proposed and used for the piloting. These techniques ensure a good tradeoff between error and robustness to noise ratio, and especially a good accuracy for a certain frequency range, regardless the gains setting of the algorithm. They have been used to estimate the successive derivatives of the sliding mode surface $s(t)$ and transmit them to the control block, by using an aircraft in virtual simulated environments. It is real-time virtual simulation which is close to the real world situation.

The piloting technique proposed in this work is more robust and simpler to implement than the quaternion one. It only requires information about the sliding mode surface.

II. PROBLEM STATEMENT

Through a methodology based on the confrontation of the real and the simulated worlds, the main objective of the present work is to design an autopilot based on robust controller in order to maintain the desired trajectory (Fig. 1). To achieve this objective, we use the Flight Simulator FS2004 as a simulated world environment coupled to a hardware and a software development platform. This simulator is developed by Microsoft, with several simulated aircrafts included in its airplane library.

In the first step, we chose the Zlin-142 airplane which is used in various aeronautic schools (pilot training) because its electronics, actuators, and sensors are easy to modify. In the second step, we chose the MQ-1 Predator airplane which is used in reconnaissance or attack.

The two chosen systems do not have similar aerodynamic configurations. The purpose is to demonstrate that the proposed piloting law is able to reestablish the flight after the command transmission reconnecting, especially in the very low altitudes flights.

III. CHARACTERISTICS OF THE AIRCRAFT ZLIN-142 AND THE MQ-1 PREDATOR

“AirWrench” tool gives access to flight dynamic characteristics [24]. This tool allows creating and tuning flight dynamics files description of simulated planes models. This software calculates aerodynamic coefficients based on the physical characteristics and performance of the aircraft.



Fig. 1 Real trajectory



Fig. 2 Zlin-142 and environment visualization



Fig. 3 MQ-1 Predator and environment visualization

Table I shows the characteristics of Zlin-142. The units are defined by: m=meter, deg=degree.

Table II shows the characteristics of MQ-1 Predator.

TABLE I
FS2004 AIRCRAFT SIMULATED CHARACTERISTICS ZLIN-142

Dimensions	Constant speed propeller	Moments of inertia
Length: 7.42 m	Prop diameter: 2.08 m	Pitch: 2780.0
Wingspan: 9.27 m	Prop gear ratio: 1.00	Roll: 4060.00
Wing surface area: 13.94 m ²	Tip velocity: 0.834 Mach	Yaw: 2340.0
Wing root chord: 1.50 m	Prop blades: 2	Cross: 0.00
Aspect ratio: 6.17	Beta fixed pitch: 20.00deg	
Taper ratio: 1.00	Prop efficiency: 0.870	
	Design altitude: 1524.0 m	

TABLE II
FS2004 AIRCRAFT SIMULATED CHARACTERISTICS MQ-1 PREDATOR.

Dimensions	Constant speed propeller	Moments of inertia
Length: 11.88 m	Prop diameter: 1.92 m	Pitch: 1800.0
Wingspan: 14.84 m	Prop gear ratio: 1.00	Roll: 3700.00
Wing surface area: 11.43 m ²	Tip velocity: 1.478 Mach	Yaw: 1800.00
Wing root chord: 1.55 m	Prop blades: 2	Cross: 0.00
Aspect ratio: 19.28	Beta fixed pitch: 20.00deg	
Taper ratio: 0.10	Prop efficiency: 0.870	
	Design altitude: 1524.0 m	

IV. IMPLEMENTATION OF A REAL-TIME INTERFACE BETWEEN MICROSOFT FLIGHT SIMULATOR AND THE MODULE "REAL TIME WINDOWS TARGET" OF SIMULINK/MATLAB

We design our Software to interface the simulated aircraft in Flight Simulator environment (read and write many sensors, actuators data, and parameters).

We communicate with FS2004 by using a dynamic link library called FSUIPC.dll (Flight Simulator Universal Inter-Process Communication). This library created by Peter Dowson is downloadable from his website [25], and can be installed by copying the directory (module) of FS2004. It allows external applications to read and write in and from Microsoft Flight Simulator MSFS by exploiting a mechanism for IPC (Inter-Process Communication) using a buffer of 64 Ko. The organization of this buffer is explained in the

documentation given with FSUIPC, from which Fig. 4 is taken [17].

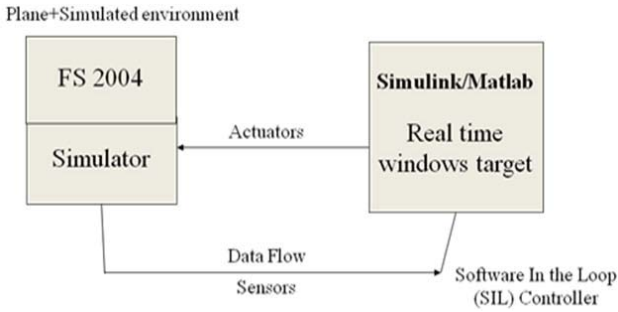


Fig. 4 Block diagram of the software environment design

To read or write a variable, we need to know its address in the table, its format, and the necessary conversions. For example, the indicated air speed is read as a signed long S32 at the address 0x02BC. The data in Table III are recorded in real time.

In Table III, the units are defined by: rad/s=radian/second, ft/s²=feet/second², meter/min=meter/minutes.

TABLE III
FLIGHT PARAMETERS IN THE BUFFER FSUIPC

Address	Name	Var.Type	Size (octet)	Usage
6010	Latitude (λ)	FLT64	8	Degree
6018	Longitude (μ)	FLT64	8	Degree
6020	Altitude (h)	FLT64	8	Meter
057C	Bank angle (ϕ)	S32	4	Degree
0578	Elevation angle (θ)	S32	4	Degree
0578	Head angle (ψ)	U32	4	Degree
30B0	Rotation rate (p)	FLT64	8	rad/s
30A8	Rotation rate (q)	FLT64	8	rad/s
30B8	Rotation rate (r)	FLT64	8	rad/s
3060	Acceleration (a_x)	FLT64	8	ft/s ²
3068	Acceleration (a_y)	FLT64	8	ft/s ²
3070	Acceleration (a_z)	FLT64	8	ft/s ²
0842	Vertical speed (Vz)	S16	2	meter/min
02BC	Speed IAS (V)	S32	4	Knot*128
2ED0	Incidence (α)	FLT64	8	Radian
2ED8	Incidence (β)	FLT64	8	Radian
0BB2	Elevator deflection (δ_e)	S16	2	-16383 to +16383
0BB6	Aileron deflection (δ_a)	S16	2	-16383 to +16383
0BBA	Rudder deflection (δ_r)	S16	2	-16383 to +16383
088C	Thrust control (δ_x)	S16	2	-16383 to +16383

In this work, the main goal is to maintain the desired aircraft's trajectory; and to do so, we propose the following approach:

- Implementation of a real time interface between the flight simulator FS2004 and the module real time Windows target of Simulink/MATLAB;
- Description and analysis of the aircraft system model;
- Development and implementation of the technique based on the combination of the robust differentiator with a dynamic adaptation of the gains and the robust controller via second order sliding mode for the design of the autopilot controller;
- Flight tests.

V. SYSTEM MODELING

The model describing the system state is [18]–[23]:

$$\dot{x} = f(x) + g(x)U \quad (1)$$

With x the aircraft state vector in the body frame:

$$x = [u \ v \ w \ p \ q \ r \ \phi \ \theta \ \psi]^T \quad (2)$$

$$= [x_1 \ \dots \ x_9]^T$$

$U = [\delta_t \ \delta_e \ \delta_a \ \delta_r]^T$ the control vector and δ_t , δ_e , δ_a and δ_r denoting thrust control, elevator deflection, aileron deflection and rudder deflection.

The nonlinear functions $f(x)$ and $g(x)$ are given by [23]:

$$f(x) = [f_1(x) \ \dots \ f_9(x)]^T \quad (3)$$

where:

$$f_1(x) = x_2x_6 - x_3x_5 + C_{x_2}x_5 + C_{x_4} + C_{x_5}\alpha + C_{x_1}\dot{\alpha} - g\sin x_8$$

$$f_2(x) = x_3x_4 - x_1x_2 + C_{y_2}x_4 + C_{y_3}x_6 + C_{y_6}\beta + C_{y_1}\dot{\beta} + C_{y_7} + g\sin x_9 \cos x_8$$

$$f_3(x) = x_1x_5 - x_2x_4 + C_{z_2}x_5 + C_{z_4} + C_{z_4} + C_{z_5}\alpha + C_{z_1}\dot{\alpha} + g\cos x_9 \cos x_8$$

$$f_4(x) = -\frac{I_{zz}}{\Delta} [-I_{xz}x_4x_5 + (I_{yy} - I_{zz})x_6x_5 + C_{l_2}x_4 + C_{l_3}x_6] - \frac{I_{xz}}{\Delta} - \frac{1}{\Delta} [-I_{zz}(C_{l_5}\beta + C_{l_1}\dot{\beta} + C_{l_7}) - I_{xz}(C_{n_6}\beta + C_{n_1}\dot{\beta})]$$

$$f_5(x) = \frac{1}{I_{yy}} (I_{zz} - I_{xx})x_4x_6 + I_{xz}(x_6^2 - x_4^2) + C_{m_2}x_5 + C_{m_5}\alpha + C_{m_1}\dot{\alpha} + C_{m_4}$$

$$f_6(x) = -\frac{I_{xz}}{\Delta} [I_{xz}x_4x_5 - I_{xx}(I_{yy} - I_{zz})x_6x_5 - C_{l_2}x_4 - C_{l_3}x_6] - \frac{I_{xx}}{\Delta} [I_{xz}x_6x_5 + (I_{yy} - I_{xx})x_4x_5 + C_{n_2}x_4 + C_{n_3}x_6] - \frac{1}{\Delta} [-I_{zz}(C_{l_5}\beta + C_{l_1}\dot{\beta} + C_{l_7}) + I_{xx}(C_{n_6}\beta + C_{n_1}\dot{\beta}) + C_{n_7}]$$

$$f_7(x) = x_4 + x_5 \sin x_7 \tan x_8 + x_6 \cos x_7 \tan x_8$$

$$f_8(x) = x_5 \cos x_7 - x_6 \sin x_7$$

$$f_9(x) = \frac{x_5 \cos x_7 + x_6 \sin x_7}{\cos x_8}$$

$$g(x) = \begin{bmatrix} \frac{F_{prop} \cos \alpha_m}{m} & C_{x3} & 0 & 0 \\ 0 & 0 & C_{y4} & C_{y5} \\ \frac{F_{prop} \sin \alpha_m}{m} & C_{z3} & 0 & 0 \\ 0 & 0 & a_1 & a_2 \\ 0 & C_{m3} & 0 & 0 \\ 0 & 0 & a_3 & a_4 \\ 0 & 0 & 0 & 0 \\ 0 & 0 & 0 & 0 \\ 0 & 0 & 0 & 0 \end{bmatrix}$$

where:

$$\Delta = I_{xz}^2 - I_{xx}I_{zz},$$

$$a_1 = -\frac{(I_{zz}C_{l4} - I_{xz}C_{n4})}{\Delta},$$

$$a_2 = -\frac{(I_{zz}C_{l6} - I_{xz}C_{n5})}{\Delta},$$

$$a_3 = -\frac{(I_{xx}C_{n4} - I_{xz}C_{l4})}{\Delta},$$

$$a_4 = -\frac{(I_{zz}C_{n5} - I_{xz}C_{l6})}{\Delta}$$

The coefficients $C_{x1}, C_{x2}, \dots, C_{m3}$ are defined in Table IV [23].

The changing mass $m(t)$ is

$$m(t) = m_0(t) - c \cdot t \tag{4}$$

$$m_0(t) = m_{aircraft} - m_{fuel}$$

is the total weight equal to 1090 kg for the Zlin-142 and 581 kg for the MQ-1 Predator, $c(t)$ is the cumulated fuel consumption.

The following condition must always hold:

$$m_{fuel} - c(t) \geq 0.$$

The aircraft motor position has a pitch and a yaw offset orientation angles. In the case of our aircrafts, the pitch setting is $\alpha_m = 0,349$ radian = 20°, and the yaw setting is $\beta_m = 0$. The engine propulsion force is written in the body frame reference [15]:

$$F = F_{prop} \begin{pmatrix} \cos \beta_m \cos \alpha_m \\ \sin \beta_m \\ \cos \beta_m \sin \alpha_m \end{pmatrix} \sigma_t = \frac{K_m \rho}{V_a} \tag{5}$$

V_a is the aerodynamic velocity, K_m is a constant, and σ_t is the throttle position (between 0.0 and 1.0).

TABLE IV
EXPRESSION OF THE MODIFIED AERODYNAMIC COEFFICIENTS

$C_{x1} = \frac{QSC_{x\dot{\alpha}}}{m}$	$C_{x2} = \frac{QScC_{x\alpha}}{mV}$	$C_{x3} = \frac{QSc_{x\delta_e}}{m}$
$C_{x4} = \frac{QSC_{x0}}{m}$	$C_{x5} = \frac{QScC_{x\alpha}}{mV}$	$C_{y1} = \frac{QsbC_{y\beta}}{2mV}$
$C_{y2} = \frac{QsbC_{yp}}{2mV}$	$C_{y3} = \frac{QsbC_{yr}}{2mV}$	$C_{y4} = \frac{QSc_{y\delta_a}}{m}$
$C_{y5} = \frac{QSc_{y\delta_r}}{m}$	$C_{y6} = \frac{QSc_{y\beta}}{m}$	$C_{z1} = \frac{QScC_{z\dot{\alpha}}}{m}$
$C_{z2} = \frac{QScC_{zq}}{mV}$	$C_{z3} = \frac{QScC_{m\delta_e}}{m}$	$C_{z4} = \frac{QScC_{z0}}{m}$
$C_{z5} = \frac{QScC_{z\alpha}}{m}$	$C_{l1} = \frac{Qsb^2C_{l\beta}}{2V}$	$C_{l2} = \frac{Qsb^2C_{yp}}{2V}$
$C_{l3} = \frac{Qsb^2C_{lr}}{2V}$	$C_{l4} = QsbC_{l\delta_a}$	$C_{l5} = QsbC_{l\beta}$
$C_{l6} = QsbC_{l\delta_r}$	$C_{l7} = QsbC_{l0}$	$C_{m1} = \frac{Qsc^2C_{m\dot{\alpha}}}{V}$
$C_{m2} = \frac{Qsc^2C_{mq}}{V}$	$C_{m3} = \frac{QscC_{m\delta_e}}{I_{yy}}$	$C_{m4} = QscC_{m0}$
$C_{m5} = QscC_{m\alpha}$	$C_{n1} = \frac{Qsb^2C_{n\beta}}{2V}$	$C_{n2} = \frac{Qsb^2C_{np}}{2V}$
$C_{n3} = \frac{Qsb^2C_{nr}}{2V}$	$C_{n4} = QsbC_{n\delta_a}$	$C_{n5} = QsbC_{n\delta_r}$
$C_{n5} = QsbC_{n\delta_r}$	$C_{n6} = QsbC_{n\beta}$	$C_{n7} = QsbC_{n0}$

VI. ANALYSIS OF THE PILOTING

The aircraft dynamic analysis confirms that Roll and Yaw moments equations $f_4(x)$ and $f_6(x)$ have the same shape and they are similar. This observation enforces us to find a control method which allows avoiding the singularity problem. In order to do so, we propose to control the longitudinal speed u by the thrust control δ_t , the bank angle φ by the aileron deflection δ_a , the pitch angle θ by the elevation deflection δ_e and the azimuthal angle ψ by the aileron and elevation deflections δ_a, δ_e . The rudder deflection δ_r is used in the landing and the taking off. To make a turn, we use bank to turn procedure which needs aileron and elevator deflections. It is based on "human piloting techniques".

We propose the following output vector:

$$y = [u \quad \varphi \quad \theta \quad \psi]^T \tag{6}$$

The kinematic model is represented by the equations expressing $f_7(x), f_8(x)$, and $f_9(x)$. Notice that the expression of $f_9(x)$ contains a singularity when $x_8 = \pm \frac{\pi}{2}$, where the terms $\tan(x_8)$ and $\sec(x_8) = \frac{1}{\cos(x_8)}$ are infinite. Such conditions occur in aerobatic manoeuvres where the aircraft loops or climbs at a near vertical angle. Two techniques are used to overcome these problems. The pitch angle can be constrained so that the computation results in a valid floating point number. For example, $\tan(x_8) = 114.6$ and this value can be used in computations when the pitch attitude is between 89.50 and 90.50.

The numerical error introduced by this approximation only occurs at this extreme flight attitude where its effects on the aircraft behavior may not be apparent. The commonly [18]. In this work, we propose the adaptive differentiators via sliding mode because they are very robust and simpler to implement than the quaternion technique. They need only the sliding mode surface.

VII. APPLICATION OF THE ADAPTIVE DIFFERENTIATORS FOR SECOND ORDER SLIDING MODE

A. Review of High Order Sliding Mode Control

The state equations of the nonlinear system are given by:

$$\dot{x} = f(x) + g(x).U \tag{7}$$

and $S(t, x)$ is the sliding mode surface. For our case, $S = y - y_d$ where y_d is the desired output signal.

The task is to vanish the output S in finite time and to keep $S \equiv 0$.

According to the conception of system relative degree, there are two conditions [10], [20]-[22].

- Relative degree $r = 1$, if and only if $\partial \dot{S} / \partial U \neq 0$
- Relative degree $r \geq 2$, if $\partial S^{(i)} / \partial U = 0$

$$(i = 1, 2, \dots, r - 1), \text{ and } \partial S^{(r)} / \partial U \neq 0 \tag{8}$$

The aim of the first order sliding mode control is to force the state to move on the switching surface $S(t, x)$. In high order sliding mode control, the purpose is to force the state to move on the switching surface $S(t, x) = 0$ and to keep its $(m - 1)^{th}$ first successive derivatives null. In the case of second order sliding mode control, the following relation must be verified:

$$S(t, x) = \dot{S}(t, x) = 0 \tag{9}$$

In sliding mode control of arbitrary order, the core idea is that the discrete function acts on a higher order sliding mode surface and yields:

$$S(t, x) = \dot{S}(t, x) = \dots = S^{(r-1)} = 0 \tag{10}$$

We define the relative degree of system (7) as the number r when the control input U appears for the first time in the r^{th} derivative of S , $\frac{dS^{(r)}}{dU} \neq 0$.

So, the following expression can be obtained

$$S^{(r)} = a(t, x) + b(t, x).U \tag{11}$$

Therefore, high order sliding mode control is transformed to stability of r order dynamic system (7), (8). Through the Lie derivative calculation, we can directly check that [18], [13], [16].

$$\begin{aligned} b &= L_g L_f^{r-1} S = \frac{dS^{(r)}}{dU} \\ a &= L_f^r S \end{aligned} \tag{12}$$

The sliding mode equivalent control is $U_{eq} = -\frac{a(t,x)}{b(t,x)}$. At present, the aim of the control is to design a discrete feedback control, so that the new system converges into origin on the r order sliding mode surface within limited time. However, in (7), both $a(t, x)$ and $b(t, x)$ are bounded function. There are positive constants K_m, K_M and C so that [8]-[12]:

$$\begin{aligned} 0 < K_m \leq b(t, x) \leq K_M \\ |a(t, x)| \leq C \end{aligned} \tag{13}$$

B. Controller Construction

Let p be a positive number. Denote

$$\Sigma_{0,r} = S$$

$$\Sigma_{1,r} = \dot{S} + \beta_1 N_{1,r} \text{sgn}(S)$$

$$\Sigma_{i,r} = S^{(r)} + \beta_i N_{i,r} \text{sgn}(\Sigma_{i-1,r}) \quad i = 1, \dots, r - 1$$

$$N_{1,r} = |S|^{(r-1)/r}$$

$$N_{i,r} = (|S|^{p/r} + |\dot{S}|^{p/(r-1)} \dots \dots + |S^{(i-1)}|^{p/(r-i+1)})^{(r-i)/p}$$

$$N_{r-1,r} = (|S|^{p/r} + |\dot{S}|^{p/(r-1)} \dots \dots + |S^{(r-2)}|^{p/2})^{1/p} \tag{14}$$

where $\beta_1, \beta_2, \dots, \beta_{r-1}$ are positive numbers.

In the above formulae, $\text{sgn}()$ denotes the usual sign function and when the argument is a vector, then $\text{sgn}()$ denotes a vector whose elements are the signs of the argument's elements.

Theorem 1. [6]-[8], [12] Let system (7) have relative degree r with respect to the output S and (13) be fulfilled. Then with properly chosen positive parameters $\beta_1, \beta_2, \dots, \beta_{r-1}$ controller

$$U = -\gamma. \text{sgn}(\Sigma_{r-1,r}(S, \dot{S}, \ddot{S}, \dots, S^{(r-1)})) \tag{15}$$

provides for the appearance of r -sliding mode $S \equiv 0$ attracting trajectories in finite time.

Certainly, the number of choices of β_i is infinite. Here are a few examples with β_i tested for $r \leq 3$, p being the least common multiple of $1, 2, \dots, r$.

The sliding mode controller is given:

- 1) $U = -\gamma. \text{sgn}(S)$
 - 2) $U = -\gamma. \text{sgn}(\dot{S} + |\dot{S}|^{1/2} \text{sgn}(S))$
 - 3) $U = -\gamma. \text{sgn}\left(\ddot{S} + 2.(|\dot{S}|^3 + |S|^2)^{1/6} . \text{sgn}(\dot{S} + |\dot{S}|^{2/3} . \text{sgn}(S))\right)$
- (16)

From (16), we can also see that, when $r=1$, the controller is traditional relay sliding mode control; when $r=2$, in fact, the controller is a super twisting algorithm of second order sliding mode.

Getting the differentiation of a given signal is always essential in automatic control systems. We often need to differentiate a variable or a function. So there are a lot of numerical algorithms for this issue. The same situation appears in the design of high order sliding mode controller (16) that needs to calculate the derivative values of sliding mode variable.

C. Differentiators for Higher Order Sliding Mode

For the sliding mode algorithm, higher gains values can improve accuracy, but this leads to an amplification of noise in

the estimated signals. The compromise between these two criteria (accuracy, robustness to noise ratio) is difficult to achieve. On the one hand, the gains values must increase in order to derive a signal sweeping of certain frequency ranges. On the other hand, low gains values must be imposed to reduce the noise amplification. Our goal is to develop a differentiation algorithm in order to have a good compromise between error and robustness to noise ratio, especially to guarantee, regardless of the gains setting of the algorithm, a good accuracy for certain frequency ranges. To satisfy at best these criteria, we propose a new version of the differentiators of higher order sliding modes with a dynamic adaptation of the gains:

- Second-order differentiator for the control of the Euler angles φ , θ , and ψ ;
- First order differentiator for the control of longitudinal speed u .

D. For the Euler Angles φ , θ , and ψ

The relative degrees are:

$$r_\varphi = r_\theta = r_\psi = 2$$

The control input can be chosen as:

$$U = -\gamma \cdot \text{sgn}(\dot{S} + |S|^{1/2} \cdot \text{sgn}(S)) \quad (17)$$

where

$$\begin{aligned} U &= [\delta_e \quad \delta_a \quad \delta_r]^T \\ S &= [S_\varphi \quad S_\theta \quad S_\psi]^T \\ \gamma &= \begin{bmatrix} \gamma_\varphi & 0 & 0 \\ 0 & \gamma_\theta & 0 \\ 0 & 0 & \gamma_\psi \end{bmatrix} \end{aligned} \quad (18)$$

We propose the sliding mode surfaces from the differentiator:

$$\begin{cases} S_0 = z_0 - y_d \\ S_1 = z_1 - v_0 \\ S_2 = z_2 - v_1 \end{cases} \quad (19)$$

where the desired vector state variables and the outputs of the differentiator are defined by:

$$\begin{cases} y_d = [\varphi_d \quad \theta_d \quad \psi_d]^T \\ z_0 = [z_{0\varphi} \quad z_{0\theta} \quad z_{0\psi}]^T \\ z_1 = [z_{1\varphi} \quad z_{1\theta} \quad z_{1\psi}]^T \\ z_2 = [z_{2\varphi} \quad z_{2\theta} \quad z_{2\psi}]^T \end{cases} \quad (20)$$

v_0 and v_1 are given by the adaptive second order differentiator.

$$\begin{cases} \dot{z}_0 = v_0 \\ v_0 = -\hat{\lambda}_0 |S_0|^{3/4} \text{sgn}(S_0) - K_0 S_0 + z_1 \\ \dot{z}_1 = v_1 \\ v_1 = -\hat{\lambda}_1 |S_1|^{3/2} \text{sgn}(S_1) - K_1 S_1 + z_2 \\ \dot{z}_2 = v_2 \\ v_2 = -\hat{\lambda}_2 |S_2|^{1/2} \text{sgn}(S_2) - \hat{\lambda}_3 \int_0^t \text{sgn}(S_2) dt - K_2 S_2 \end{cases} \quad (21)$$

where K_1 , K_2 , $K_3 > 0$.

The dynamic adaptation of the gains $\hat{\lambda}_i$, $i \in \{0,1,2\}$ are given by:

$$\begin{cases} \dot{\hat{\lambda}}_1 = |S_0|^{3/4} \text{sgn}(S_0) S_0 \\ \dot{\hat{\lambda}}_2 = |S_1|^{3/2} \text{sgn}(S_1) S_1 \\ \dot{\hat{\lambda}}_3 = |S_2|^{1/2} \text{sgn}(S_2) S_2 \\ \hat{\lambda}_3 = S_2 \int_0^t \text{sgn}(S_2) dt \end{cases} \quad (22)$$

In case of using the differentiator, variable S is considered as given input of the differentiator. Then, the output of differentiator z can be used to estimate corresponding order derivative of S (Fig. 5).

The reduction of the noise is assumed by the presence of the linear term $K_i S_i$ in the equation of each output i of the adaptive algorithm. This linear term can be expressed as the law of the equivalent control which allows the reduction of the chattering effect. The addition of this continuous term smoothen the output noise due to a low gain values. If the chosen values of these gains become very low, the convergence time of the algorithm becomes slow. Therefore, the choice of the convergence gains remains difficult and is based on a compromise between reduction of the noise and the convergence time of the adaptive differentiator. It should also be noted that in the presence of noise, it is necessary to impose the small initial values of the dynamic gains to reduce the effect of the discontinuous control. Moreover, the presence of integral term in the expressions of the dynamic gains provides also the smoothing of the estimated derivatives.

The application of the differentiators with dynamic adaptation of the gains via sliding mode controller in FS2004 is shown in Fig. 5.

E. Simulation Results

We run the Flight Simulator FS2004 and the interface with the module Real Time Windows Target of Simulink/MATLAB.

The aircrafts' taking off were done using the keyboard. Then, we run our software to transmit the control inputs based on the adaptive differentiators via second order sliding mode to the autopilot controller in order to maintain the desired trajectory.

The input signals to the upper and lower saturation values of the control laws are used to respect the actuators bounds. Scaled functions are added to take into account the actuators resolutions.

The robust differentiator via sliding mode technique is used to recover the desired signal. Several flight tests were realized to demonstrate the effectiveness of the combined controller/differentiator.

We chose the parameters $K_{0,i} = 50$ and $K_{1,i} = 50$, where $i = \varphi, \theta, \psi$.

The followed scenario during the flight tests at very low altitudes is summered as:

- Disconnection of the transmission for 5 to 10 seconds.
- Reestablishing the transmission.

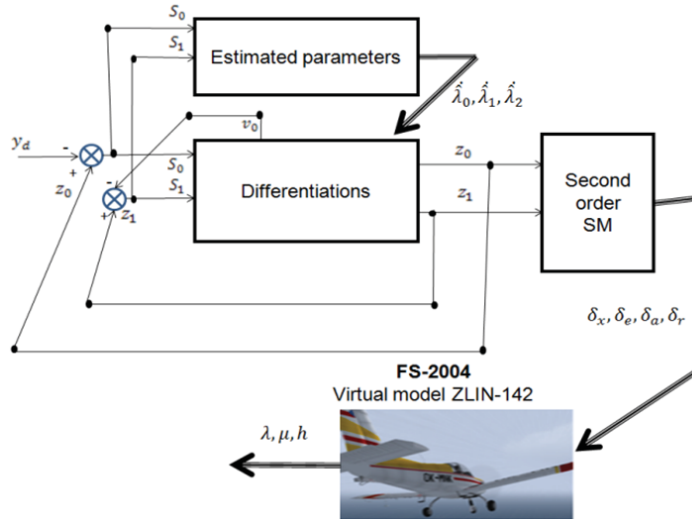


Fig. 5 Application of the adaptive differentiators for sliding mode controller in FS2004

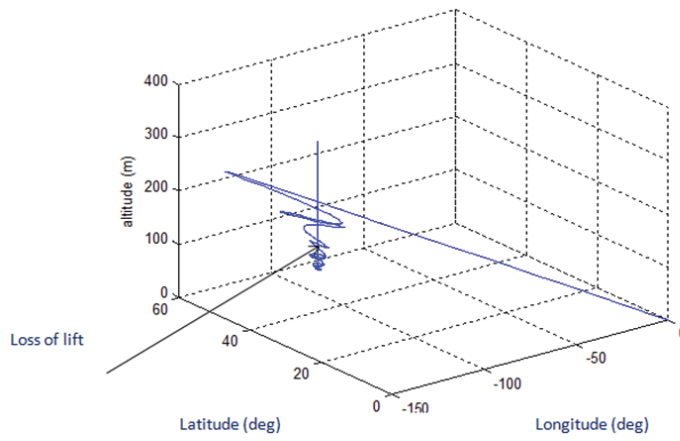


Fig.6 Apparition of the stall phenomenon in very low altitudes

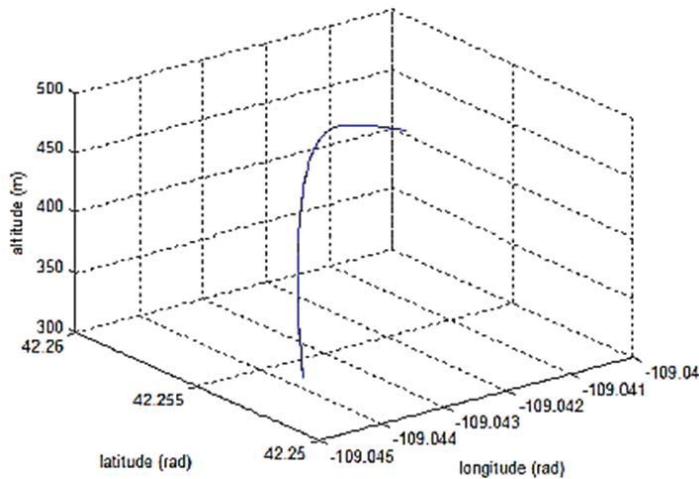


Fig. 7 MQ-1 Predator system trajectory after reestablishing the transmission at very low altitudes

The obtained results confirm that the Zlin-142 aircraft executes the flight commands and continues flying normally

for upper than altitudes of 200 meters, in other cases (altitude lesser than 200 meters) Fig. 6 shows the stall phenomenon of

the system.

We have performed the same flight tests at very low altitudes as in the precedent case but by using the MQ-1 Predator. The simulation results show that the system reestablishing its normal flight whatever the altitude is (see Fig. 7).

In the following statement, we present the simulation results of the proposed piloting low for the MQ-1 Predator flying in FS2004.

The desired signal injected and the output differentiators are shown in Fig. 8.

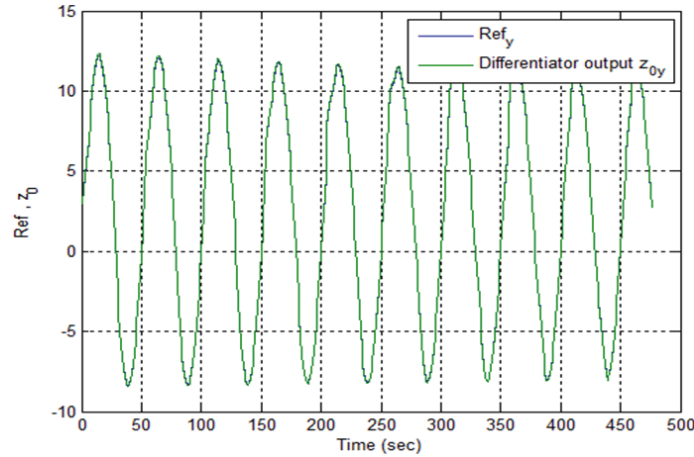


Fig. 8 Reference and output differentiator

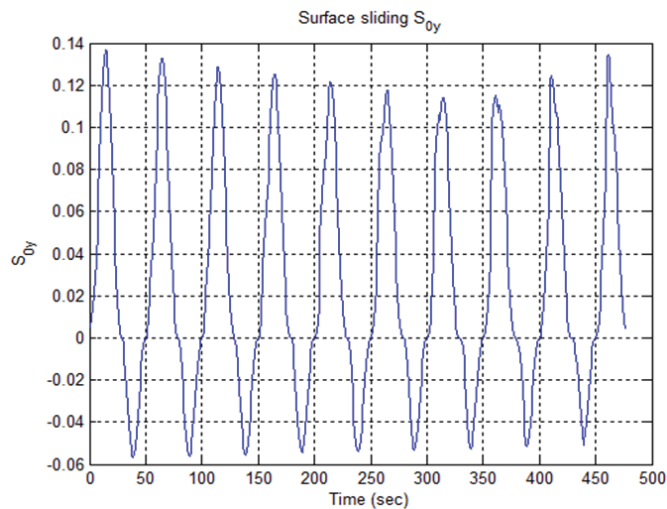


Fig. 9 Surface sliding S_0

We notice that the outputs of the differentiators $z_{0,j}$ where $j = \varphi, \theta, \psi$ follow the references φ_d, θ_d and ψ_d perfectly.

The surfaces sliding mode $S_{0\varphi, \theta, \psi}$ are small (see Fig. 9).

Fig. 10 shows the error between the output differentiator z_1 and v_0 . The signal z_1 follows v_0 .

The input signals to the upper and the lower saturation values of the aileron, rudder and elevator deflections are used to respect the virtual Joystick (PPjoy) bounds. Upper limit: 62767, lower limit: 1.

The surface sliding mode S_1 is shown in Fig. 11.

Airwrench gives the following data:

- Aileron parameters: Aileron area 1.30 m^2 , aileron up angle limit 28 degree, aileron down angle limit 20degree.

- Elevator parameters: Elevator area 2.23 m^2 , Elevator up angle limit 32 degree, Elevator down angle limit 30 degree.
- Rudder parameters: Rudder area 0.72 m^2 , Rudder angle limit 22 degree.

The aileron, elevator and rudder deflections are shown in Figs. 12-14. We notice the absence of the chattering phenomenon.

The flight tests demonstrate the robustness of the differentiator via second order sliding mode. It makes it possible to ensure a better derivation of the desired input signal in real time and this to ensure a good accuracy of tracking the desired trajectory.

F. For the Control of the Longitudinal Speed u

The relative degree is:

$$r_u = 1$$

The control input can be chosen as:

$$\delta_t = -\gamma \cdot \text{sgn}(S_{0u}) \quad (23)$$

where $S_{0u} = z_{0u} - u_d$ and $\gamma > 0$.

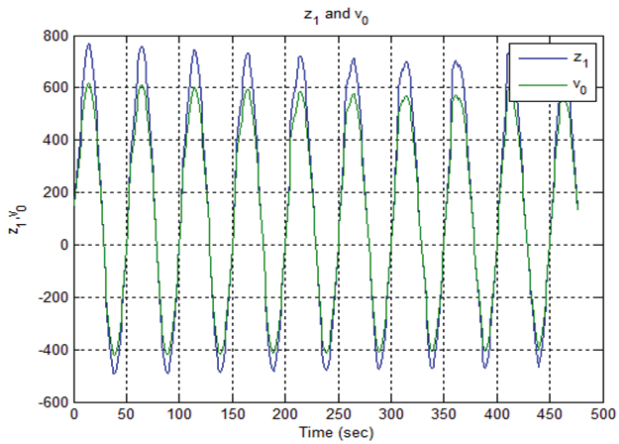


Fig. 10 Output differentiator z_1 and signal v_0 .

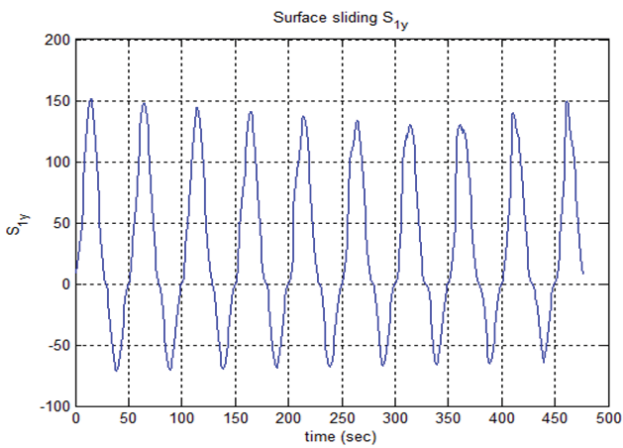


Fig. 11 Surface sliding mode S_1

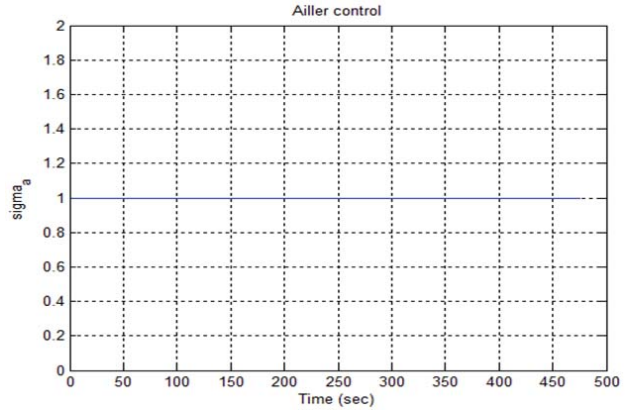


Fig. 12 Ailler control

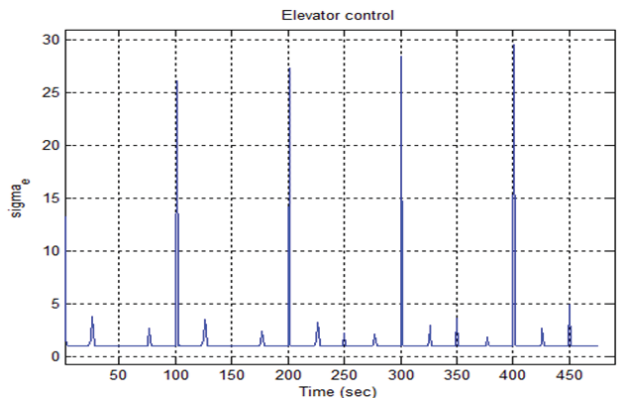


Fig. 13 Elevator control

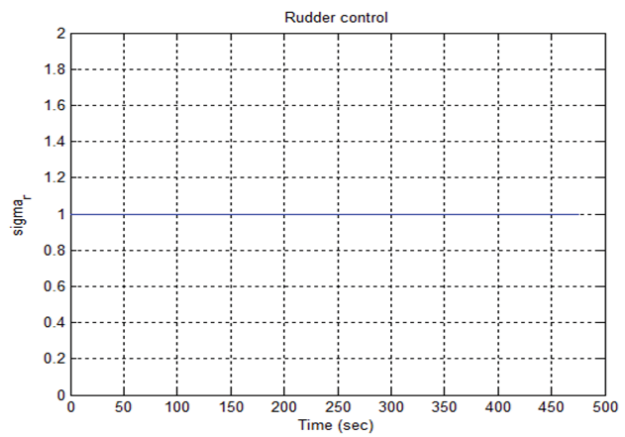


Fig. 14 Rudder control

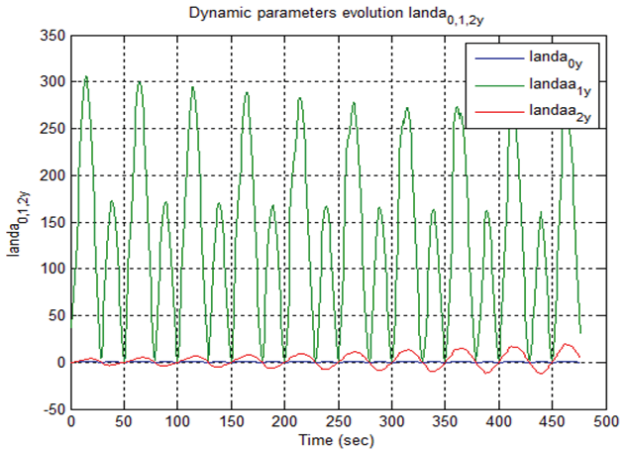


Fig. 15 Dynamic parameters evolution

We propose the adaptive super twisting:

$$\begin{cases} \dot{z}_{0u} = v_{0u} \\ v_{0u} = -\hat{\lambda}_{0u}|S_{0u}|^{\frac{1}{2}}\text{sgn}(S_{0u}) - K_u S_{0u} + z_{1u} \\ \dot{z}_{1u} = v_{1u} \\ v_{1u} = -\hat{\lambda}_{1u} \int_0^t \text{sgn}(S_{0u}) dt \end{cases} \quad (24)$$

where $K_u > 0$.

The dynamic adaptations of the gains are given by:

$$\begin{cases} \dot{\hat{\lambda}}_{0u} = |S_{0u}|^{\frac{1}{2}}\text{sgn}(S_{0u})S_{0u} \\ \dot{\hat{\lambda}}_{1u} = S_{0u} \int_0^t \text{sgn}(S_{0u}) dt \end{cases} \quad (25)$$

G. Simulation Results

We chose the parameter $\gamma = 62767$.

The reference is the longitudinal speed u expressed in m/s. We notice the presence of the error between the reference and the output differentiator (Fig. 16). This error varies between 1.8 and 6 m/s (Fig. 17).

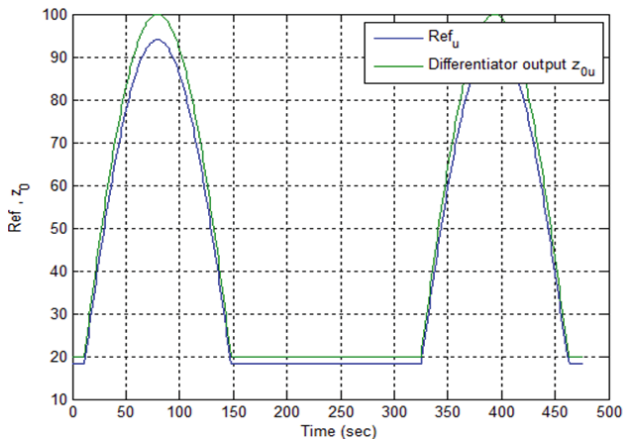


Fig. 16 Reference and output differentiator

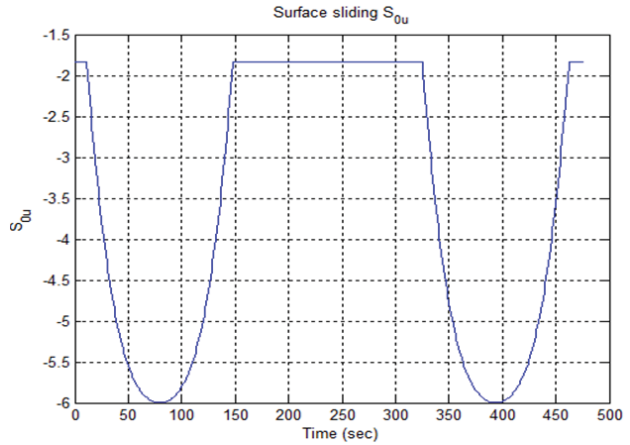


Fig. 17 Surface sliding mode S_{0u}

We notice that they increase gradually with the variation of the surface S_{0u} .

The simulations results are:

- The output differentiator follows the reference;
- The tracking error is acceptable;
- Absence of the chattering phenomenon.

VIII. CONCLUSION

In this paper, a combination of the robust differentiator with a dynamic adaptation of the gains and the robust controller via second order sliding mode for an aircraft autopilot has been presented. Our approach uses the environment simulator (FS2004) to reduce the design process complexity.

Two different systems were used to test the proposed piloting law robustness.

The MQ-1 is considered as a reconnaissance and intelligence system. Its aerodynamic configuration allows it to perform the piloting commands during very low altitudes flights once the transmission from the ground is reestablished. Its fuselage's shape reduces the drag and its control surfaces dimensioning allows the creation of the sufficient lift needed to be stabilized.

The aircraft dynamic analysis confirms that Roll and Yaw moments equations are similar and have the same shape. This observation enforced us to find a method of control which permits avoiding the singularity problem. To solve this problem, we proposed a new version of the differentiators for higher order sliding modes with a dynamic adaptation of the gains approach. This technique is more robust and simpler to implement than the quaternion one and only needs the information about the sliding mode surface.

The first order Sliding mode autopilot controller is characterized by its robustness and takes account of model uncertainties and external disturbances. Unfortunately, the application of this control law is confronted to the serious problem of the chattering phenomenon. To prevent this drawback, adaptive differentiators for the second order sliding mode controller were designed and applied.

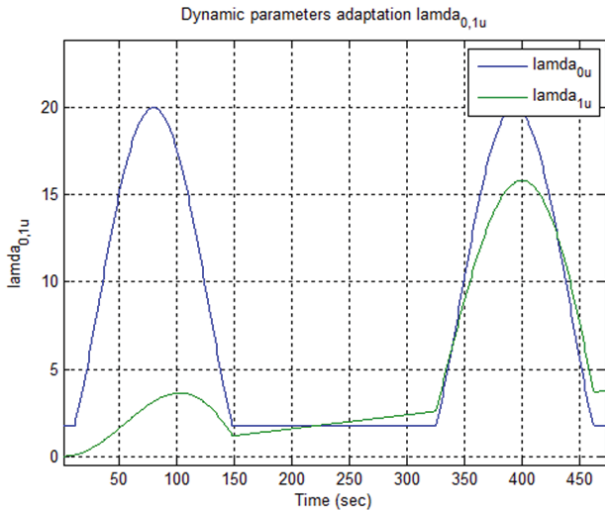


Fig. 18 Dynamic parameters evolution

For sliding mode algorithm, choosing higher gain values can improve accuracy but this leads to an amplification of noise in the estimated signals. The compromise between these two criteria (accuracy, robustness to noise ratio) is generally difficult to achieve. On one hand, these values must increase the gains values in order to derive a signal sweeping certain frequency ranges. On the other hand, low gains values must be imposed to reduce noise amplification. Hence, we developed a differentiation algorithm in order to get a good compromise between error and robustness to noise ratio and at the same time guarantee a sufficient accuracy for a specific frequency range, regardless the gains setting of the algorithm. To satisfy at best these criteria, we have proposed a new version of the adaptive differentiators of:

- First order differentiator for the control of longitudinal speed u ;
- Second-order differentiator for the control of the Euler angles.

Consequently, using this approach we obtained the following results:

- Absence of the chattering phenomenon in the control signals inputs;
- Higher accuracy of the convergence of the system towards surface, owing to the fact that the system is governed by the expression: $S = \dot{S} = 0$.

The flight tests demonstrate the robustness of the new version adaptive differentiators for the second order sliding mode. The former ensures a better derivation of the desired input signal in real time and this ensures a good accuracy in term of tracking for a desired reference.

REFERENCES

[1] O. Harkegard, "Flight Control Design Using Backstepping", Linkopings universitet, Linkoping, Sweden, 2001.
 [2] J.J.E. Slotine, "Applied nonlinear control", Practice-Hall. 1991.
 [3] J.J.E. Slotine, "Adaptive Sliding Controller Synthesis for Nonlinear Systems", International Journal of Control, 1986.

[4] J L., Junkins, K. Subbarao, A. Verma, "Structured Adaptive Control for Poorly Modeled Nonlinear Dynamical Systems". Computer Modeling in Engineering & Sciences, Vol. 1, No. 4, pp. 99-118. 2000
 [5] V. Chiroi, L. Munteanu, I. Ursu, "On Chaos Control in Uncertain Nonlinear System". Computer Modeling in Engineering & Sciences, Vol. 72, No. 3, pp. 229-246, 2011.
 [6] A. Levant, "Higher-order sliding modes, differentiation and output feedback control". International journal of control, Vol. 76, NOS 9/10, 924-941, 2003.
 [7] A. Levant, "Robust exact differentiation via sliding mode technique". Automatica, Vol.34, No.3, pp.379-384, 1989.
 [8] A. Levant, "Quasi continuous high order sliding mode controllers", IEEE Transactions on Automatic Control, Vol. N° 11, November 2005.
 [9] A. Sabanovic, L. M. Fridman, S. Spurgeon, "Variable structure systems: from principles to implementation", The Institution of Engineering and Technology, 2004.
 [10] B. Bandyopadhyay, S. Janardhanan, "Discrete-time Sliding Mode Control: A Multirate Output Feedback Approach". Springer, 2006.
 [11] B. Bandyopadhyay, F. Deepak, K. Kyung-Soo, "Sliding Mode Control Using Novel Sliding Surfaces", Springer. 2009.
 [12] D. Allerton, "Principles of flight simulation", John Wiley and Sons, chap.3, 2009.
 [13] G. Bartolini, L. Fridman, A. Pisano, E. Usai, "Modern Sliding Mode Control Theory: New Perspectives and Applications", Springer, chap. 4, 2008.
 [14] H. Yigeng, "Robust High Order Sliding Mode Control of Permanent Magnet Synchronous Motors", Recent Advances in Robust Control - Theory and Applications in Robotics and Electromechanics, InTech., 2011.
 [15] P. Perruquetti, J. Barbot, "Sliding mode control in engineering", Marcel Dekker, 2000.
 [16] J. L. Boiffier, "The dynamics of flight: the equations", Willey, pp. 92, 1998.
 [17] P. Lopez, S. N. Nouri, «Théorie élémentaire et pratique de la commande par les régimes glissants», Springer, chap.2, 2000.
 [18] R. Louali, "Real-time characterization of Microsoft Flight Simulator 2004 for integration into Hardware In the Loop architecture", 19th Mediterranean Conference on Control and Automation, Greece, 2004.
 [19] J. Salgado, «Contribution à la commande d'un robot sous marin autonome de type torpille», Thèse de Doctorat, Université de Montpellier, 2004.
 [20] V. I. Utkin, "Sliding Mode in Control Optimization", Springer-Verlag, Berlin, 1992.
 [21] B S. Yuri, Y B. Shkolnikov, D J. Mark, "An second order smooth sliding mode control", Asian journal of control. Vol. 5, No. 4, pp. 498-504, December 2003.
 [22] W. Perruquetti, J. P. Barbot, "Sliding mode control in engineering", Marcel Dekker, 2002.
 [23] M. Zaouche, «Identification et commande robuste d'un engin aérodynamique Volant à 03 axes», Thèse doctorat, Ecole Militaire Polytechnique, Algiers, 2015.
 [24] Airwrench tool, website: www.mudpond.org/AirWrench_main.htm, GWBeckwith, 2015.
 [25] P. Dowson, FSUIPC.dll, website: www.schiratti.com/dowson.html, 2015.